Where do winds drive the Antarctic Circumpolar Current?

L. C. Allison,[1] H. L. Johnson,[2] D. P. Marshall,[3] and D. R. Munday[3]

Received 23 March 2010; revised 2 May 2010; accepted 10 May 2010; published 22 June 2010.

[1] The strength of the Antarctic Circumpolar Current (ACC) is believed to depend on the westerly wind stress blowing over the Southern Ocean, although the exact relationship between winds and circumpolar transport is yet to be determined. Here we show, based on theoretical arguments and a hierarchy of numerical modeling experiments, that the global pycnocline depth and the baroclinic ACC transport are set by an integral measure of the wind stress over the path of the ACC, taking into account its northward deflection. Our results assume that the mesoscale eddy diffusivity is independent of the mean flow; while the relationship between wind stress and ACC transport will be more complicated in an eddy-saturated regime, our conclusion that the ACC is driven by winds over the circumpolar streamlines is likely to be robust. **Citation:** Allison, L. C., H. L. Johnson, D. P. Marshall, and D. R. Munday (2010), Where do winds drive the Antarctic Circumpolar Current?, *Geophys. Res. Lett.*, *37*, L12605, doi:10.1029/2010GL043355.

1. Introduction

[2] The importance of Southern Ocean winds for driving the Antarctic Circumpolar Current (ACC) has long been recognized [e.g., *Gill*, 1968]. As well as the direct transfer of momentum which accelerates the barotropic component of the current, the winds drive a surface Ekman transport that leads to patterns of convergence and divergence to the north and south. This induces vertical motions which impact upon the ocean stratification to the north of the ACC, helping to set the baroclinic component of the current.

[3] The simple model of *Gnanadesikan* [1999] for the structure of the global pycnocline illustrates the role of Southern Ocean winds in setting the stratification of the global ocean, and hence the strength of the ACC. However, the appropriate measure of the wind stress is unclear. Possibilities include:

[4] 1. The zonally averaged wind stress at the latitude of the northern edge of Drake Passage, as suggested by *Toggweiler and Samuels* [1995] and *Gnanadesikan et al.* [2007].

[5] 2. The maximum wind stress in the southern hemisphere westerly jet.

[6] 3. The mean wind stress over the latitude band of Drake Passage [e.g., *Russell et al.*, 2006].

[7] 4. The mean wind stress over the path of the ACC.

[8] In this paper, the sensitivity of the ACC transport to wind stress forcing at different locations is explored using an ocean general circulation model (MITgcm) and a simple reduced-gravity model. The results from the reduced-gravity model are compared with theoretical predictions based on the four measures of the wind stress. We demonstrate that the most reliable predictor of the ACC transport is a weighted average of the wind stress over the circumpolar streamlines of the ACC.

2. Numerical Experiments

2.1. MITgcm

[9] We use a global ocean-only configuration of the MITgcm [*Marshall et al.*, 1997] with a coarse horizontal resolution (4° × 4°). Surface temperature and salinity are restored to the Levitus climatology on a timescale of two months and six months respectively. Wind forcing is provided by the surface wind stress climatology of *Trenberth et al.* [1990]. These forcings are applied as anually-repeating 12-month cycles. Eddies are parameterized by *Gent and McWilliams* [1990] with a constant eddy diffusivity, $\kappa_{GM} = 1000\ m^2\ s^{-1}$, and the diapycnal mixing coefficient is $\kappa_v = 3 \times 10^{-5}\ m^2\ s^{-1}$.

[10] Three experiments are performed using different land mask geometries: a control integration with the standard global land mask, an experiment in which the Indian and Pacific basins are filled in with land everywhere north of the model's latitude of the southern tip of Africa, and an experiment in which the Indian and Pacific basins are filled in with land everywhere north of the model's latitude of Cape Horn. The aim is to explore the effect of removing wind forcing over these regions. Each experiment is integrated for 20,000 model years to reach thermodynamic equilibrium.

[11] Figure 1 shows the barotropic stream function averaged over the final year of each experiment. In the control integration (Figure 1a), the model has an ACC transport of 122 Sv. Filling in the Indian and Pacific basins with land everywhere north of the southern tip of Africa (Figure 1b) reduces the ACC transport to 116 Sv. When the Indian and Pacific basins are filled in with land everywhere north of Cape Horn (Figure 1c) the ACC transport is dramatically reduced to 43 Sv. Removing the Indo-Pacific wind forcing north of Drake Passage (instead of filling in the ocean basins) also reduces the ACC transport (not shown). This result suggests that the wind stress to the north of Drake Passage latitudes may be important for setting the strength of the ACC, rather than simply the wind stress inside the Drake Passage latitude belt or at the latitude of Cape Horn.

[12] The strongest winds (in these numerical experiments, as well as in reality) are found in a latitude band to the north

[1]Department of Meteorology, University of Reading, Reading, UK.
[2]Department of Earth Sciences, University of Oxford, Oxford, UK.
[3]Atmospheric, Oceanic and Planetary Physics, University of Oxford, Oxford, UK.

0094-8276/10/2010GL043355

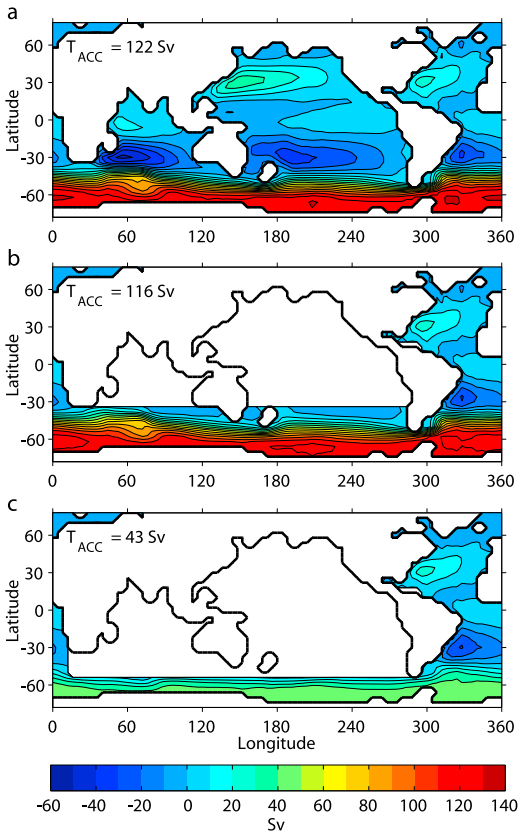

Figure 1. Barotropic stream function (Sv) in the final year of three MITgcm experiments with different land mask geometries. (a) Control experiment, (b) Indian and Pacific basins filled with land everywhere north of the southern tip of Africa, (c) Indian and Pacific basins filled with land everywhere north of Cape Horn.

of Cape Horn. In the NCEP-NCAR reanalysis [*Kistler et al.*, 2001], the maximum in the long-term mean zonally-averaged zonal wind stress is located at 52.4°S (c.f. Drake Passage latitudes: 55–63°S). The ACC exhibits a northward deflection after passing through Drake Passage, and also fans out slightly in the Indian and Pacific basins, aligning itself to some extent with the latitude of the maximum wind.

2.2. Reduced-Gravity Model

[13] Next, a 1.5-layer reduced-gravity ocean model is used to examine the sensitivity of a circumpolar current to the location of a westerly wind jet. The standard reduced-gravity equations are discretized on a C-grid with spherical geometry and a horizontal resolution of 1° × 1°. The model domain is a single sector ocean basin, 97° wide and extending from 65°N to 74°S. The Southern Ocean is represented by a zonally re-entrant channel between 56°S and the southern boundary. The dynamically-active upper layer of the model represents the light pycnocline waters of the global ocean, and the depth of the layer interface, h, can be interpreted as the depth of the global pycnocline.

[14] Mesoscale eddies are parameterized as a layer thickness diffusion following *Gent and McWilliams* [1990] with κ_{GM} = 2000 m^2 s^{-1}. The model has a constant diapycnal diffusion coefficient, $\kappa_v = 10^{-5}$ m^2 s^{-1}, which leads to a diapycnal upwelling velocity, $w^* = \kappa_v/h$. To represent surface buoyancy loss near Antarctica, the surface layer thickness is relaxed to 10 m at the southern boundary, with the relaxation decaying to zero over 4° latitude. Further details of the model are given by *Allison* [2009].

[15] The model is forced in the southern hemisphere by an idealized westerly wind jet, which has a zonal wind stress profile given by a sine squared function of latitude (Figure 2a). Nine experiments are carried out, in which the latitude of the jet axis is varied; the wind stress magnitude (0.16 N m^{-2}) and the meridional width of the jet (14° latitude) remain unchanged. In each experiment, the wind stress is constant in time, is purely zonal, and is zero away from the latitudes of the jet. The experiment with the jet in its southernmost location has the maximum wind stress centered on 62.5°S and the jet is entirely confined to the latitude band of the circumpolar channel. The

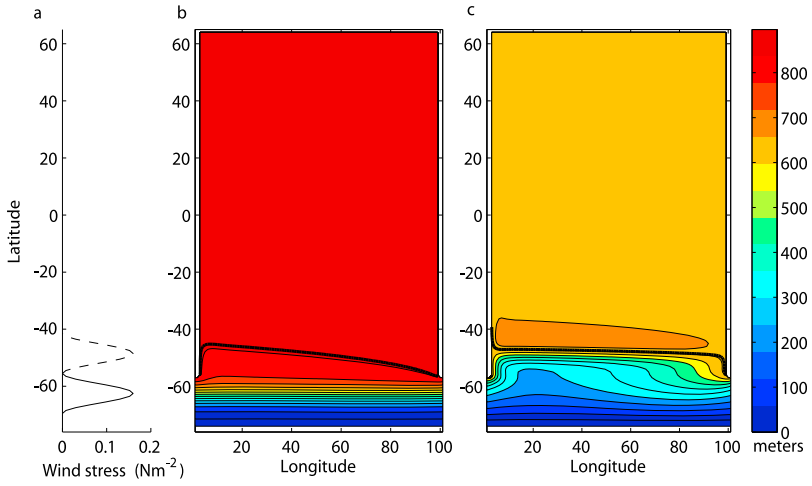

Figure 2. (a) Wind stress profiles in the reduced-gravity model experiments in which the jet is in its southernmost (solid) and northernmost (dashed) locations. (b and c) Surface layer thickness (m) in the reduced-gravity model at the end of the experiments with the wind jet in its southernmost (Figure 2b) and northernmost (Figure 2c) position. The h_{crit} layer thickness contour for each experiment is shown as a heavy black contour.

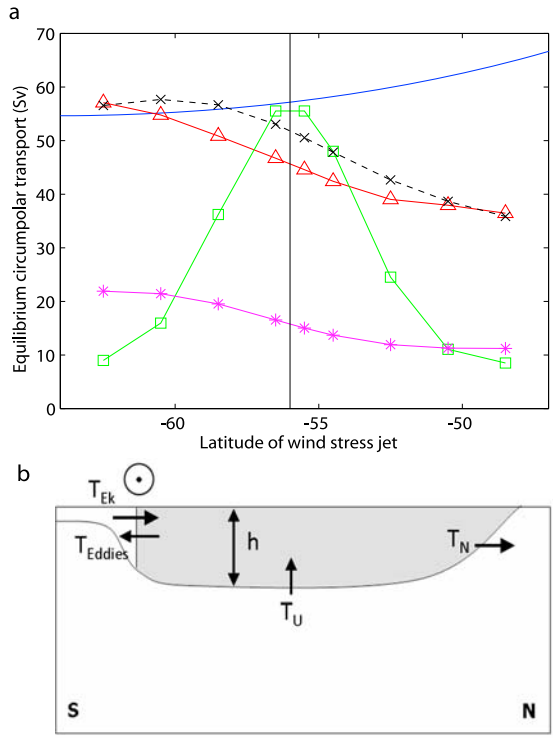

Figure 3. (a) Circumpolar transport (Sv) at the end of each reduced-gravity model experiment, with varying wind stress latitude (black crosses). Also shown are theoretical predictions for the circumpolar transport via (1) and (3) using different wind stress measures: maximum wind stress in the jet (blue curve), wind stress at the latitude of the northern edge of the channel (green squares), mean wind stress within the latitudes of the channel (magenta stars), and weighted average wind stress over the region of circumpolar streamlines (red triangles). The solid black line indicates the latitude of the northern edge of the model's circumpolar channel. (b) Schematic summarizing the pycnocline theory of *Gnanadesikan* [1999].

northernmost location has the wind stress maximum centered on 48.5°S, so that the jet is entirely within the basin to the north.

[16] For each experiment, the model is integrated for 4000 years to reach equilibrium. Details of the spin-up process are discussed by *Allison* [2009]. At the end of each integration the layer interface is near to the surface at the southern boundary, slopes downwards across the circumpolar current, and is flat within the basin to the north. Shown in Figures 2b and 2c are the surface layer thickness at the end of the model experiments in which the wind jet is in its southernmost and northernmost locations. The circumpolar current can be identified by the region in which the meridional gradient in layer thickness is large. In the experiment with the northward-shifted wind jet, the surface layer within the basin is shallower than in the experiment with the jet in its southernmost location.

[17] Figure 3a shows the zonal volume transport through the model's representation of Drake Passage at the end of each experiment (black crosses). In the experiments in which the wind jet is located further north, the model has a weaker circumpolar transport. In the following section, this result will be compared with theoretical predictions for the circumpolar transport using different measures of the Southern Ocean wind stress.

3. Theory

3.1. Gnanadesikan's Pycnocline Model

[18] A simple analytical theory relating the depth of the global pycnocline to processes which alter the volume of the light pycnocline waters was proposed by *Gnanadesikan* [1999] and is summarized in Figure 3b. In the Southern Ocean, the northward Ekman transport, T_{Ek}, leads to a deepening of the global pycnocline, while mesoscale eddies counteract this by reducing the pycnocline slope via an effective southward transport, T_{Eddies}. Diapycnal mixing in the basins to the north deepens the pycnocline by producing an upwelling transport, T_{U}. *Gnanadesikan* [1999] also includes deep water formation in the North Atlantic, T_{N}, which may influence the strength of the ACC [*Fučkar and Vallis*, 2007], but this is neglected in the present study.

[19] Associated with the strong thermal wind component of the ACC, isopycnals slope steeply downwards to the north across the current. The baroclinic transport of the ACC can therefore be linked through geostrophic balance to the depth of the pycnocline:

$$T_{\mathrm{ACC}} \approx -\frac{g'}{2f_0}\left(h_{\mathrm{N}}^2 - h_{\mathrm{S}}^2\right) \approx -\frac{g' h_{\mathrm{N}}^2}{2f_0}. \tag{1}$$

Here $g' = g\Delta\rho/\rho_0$ is the reduced gravity (where g is the gravitational acceleration and $\Delta\rho/\rho_0$ is the fractional density difference between the pycnocline layer and the abyss), f_0 is the Coriolis parameter (negative in the Southern Ocean), and h_{N} and h_{S} are the pycnocline depth to the north and south of the model Drake Passage.

[20] At equilibrium the processes which affect the volume of the pycnocline waters, and hence the ACC transport, are in balance [*Gnanadesikan*, 1999]:

$$\frac{-\tau_{\mathrm{ACC}} L_x}{\rho_0 f_0} - \frac{\kappa_{\mathrm{GM}} L_x h_{\mathrm{N}}}{L_y} + \frac{\kappa_{\mathrm{v}} A}{h_{\mathrm{N}}} = 0. \tag{2}$$

Here the terms on the left hand side represent T_{Ek}, T_{Eddies} and T_{U} respectively, using the scalings of *Gnanadesikan* [1999], where A is the surface area of the basin, L_x is a zonal length scale for the Southern Ocean, L_y is a length scale for the width of the ACC, and τ_{ACC} is a measure of the wind stress (to be determined), with its appropriate value of f_0. The equilibrium pycnocline depth is given by

$$h_{\mathrm{N}} = \frac{\frac{-\tau_{\mathrm{ACC}} L_x}{\rho_0 f_0} + \sqrt{\left(\frac{\tau_{\mathrm{ACC}} L_x}{\rho_0 f_0}\right)^2 + 4\kappa_{\mathrm{v}} A\left(\frac{\kappa_{\mathrm{GM}} L_x}{L_y}\right)}}{2\left(\frac{\kappa_{\mathrm{GM}} L_x}{L_y}\right)}. \tag{3}$$

3.2. Wind Stress Measures

[21] The simplest measure of the zonal wind stress, τ_{ACC}, is the maximum of the westerly jet, which in the reduced-gravity model is 0.16 N m^{-2} in every experiment. If L_x and f_0 are evaluated at the latitude of the maximum wind stress, then as the wind jet shifts northward L_x increases and the magnitude of f_0 decreases. The blue curve in Figure 3a shows the theoretical circumpolar transport estimate from

(1) and (3) for varying wind stress latitude, when τ_{ACC} is fixed at 0.16 N m^{-2}. Using this measure of the wind stress leads to an increasing circumpolar transport estimate as the wind jet is shifted northward: a response which is the opposite sign to the results from the reduced-gravity model experiments.

[22] It is commonly assumed that the Southern Ocean Ekman transport is set by the mean wind stress at the latitude of the northern edge of Drake Passage [e.g., *Toggweiler and Samuels*, 1995; *Gnanadesikan et al.*, 2007]. The green squares in Figure 3a show the theoretical circumpolar transport calculated via (1) and (3) for the wind stress profile in each model experiment, using the wind stress at the latitude of the northern edge of the circumpolar channel. This measure leads to a good estimate of the circumpolar transport (close to the model result) when the center of the wind stress jet is located close to the northern edge of the channel, but a vastly underestimated circumpolar transport when the center of the jet is located elsewhere.

[23] Also shown in Figure 3a (magenta stars) is the theoretical prediction for the equilibrium circumpolar transport when T_{Ek} is calculated using the mean wind stress within the latitudes of the circumpolar channel. This method captures the decrease in transport as the wind jet is shifted equatorward, but it consistently underestimates its absolute value.

[24] It is clear from Figure 2 that as the wind jet is shifted equatorward, the circumpolar current adjusts its position to align with the wind stress, except where it is forced to deviate poleward to pass through the model's representation of Drake Passage. The circumpolar current is therefore influenced by wind stress outside the latitudes of the channel (as evident in the MITgcm experiments in Figure 1). In the layer thickness field from the experiment with the northernmost wind jet there is also evidence of a gyre circulation within the basin; when part of the wind jet is located to the north of the channel, some of the wind stress spins up a gyre, rather than the circumpolar current. The fraction of the wind stress which imparts momentum into the circumpolar current (rather than a gyre) must be identified.

[25] The northern limit of the circumpolar current can be defined by the layer thickness contour $h_{crit} = 0.99\ h_e$, where h_e is the surface layer thickness on the eastern boundary of the basin. The h_{crit} contour represents the deepest layer thickness contour which passes through the circumpolar channel. It is shown for both layer thickness fields in Figure 2 as a heavy black contour. To the south of this contour, the wind stress imparts momentum into the circumpolar current and drives a northward Ekman transport which deepens the pycnocline to the north. Everywhere north of the h_{crit} contour, the wind stress simply redistributes volume within the surface layer in the basin. To obtain the net meridional transport which sets the depth of the pycnocline and the strength of the circumpolar current, we must integrate the sum of the Ekman and eddy transports over circumpolar streamlines, between the southern limit of the current and the h_{crit} contour. We assume that the flow is nearly zonal and the combined meridional transport does not vary significantly across the ACC. The wind stress, τ_{ACC}, is then given by

$$\frac{\tau_{ACC}}{f_0} = \frac{1}{L_x L_y} \iint_{south}^{h_{crit}} \frac{\tau^{(x)}(x,y)}{f(y)}\, dA, \qquad (4)$$

where $\tau^{(x)}(x, y)$ is the full zonal wind stress field, L_y (which also affects T_{Eddies}) is the mean meridional distance between the h_{crit} contour and the southern limit of the circumpolar current, $f(y)$ is the latitudinally-varying Coriolis parameter and f_0 is its reference value in the Southern Ocean. Note that f_0 and L_x are both cancelled when this expression is substituted into (2).

[26] The red triangles in Figure 3a show the theoretical circumpolar transport obtained using this wind stress measure to calculate T_{Ek}. The theory now captures the decrease in transport as the wind jet is shifted equatorward, and the magnitude of the transport predicted by the theory is in much better agreement with the model results. The transport reduction with northward-shifted winds results from a decrease in T_{Ek} through a subtle balance between a decrease in area-integrated wind stress and an increase in L_y, although the latter also reduces T_{Eddies}.

4. Discussion

[27] This study has identified the measure of the zonal wind stress which sets the transport of the ACC, by considering the link between ACC transport and the global ocean stratification. The best predictor of the ACC transport in our model was found to be a weighted average of the wind stress over the circumpolar streamlines of the ACC, taking into account its northward deflection.

[28] This result also has relevance for understanding past and future climate change: the winds over this region play a role in setting the stratification of the global ocean, with implications for carbon uptake, biogeochemistry and ocean heat content.

[29] It is important to note that the link between ACC transport and the global stratification applies only to the baroclinic component of the transport, and holds on centennial timescales and longer. The results of this study therefore apply to the steady state of the ACC and variations on long timescales. Transport variability on shorter timescales is likely to be driven by changes in wind stress over different regions of the Southern Ocean. For instance, the southern mode of barotropic ACC variability highlighted by *Hughes et al.* [1999] is mainly influenced by winds to the south of Drake Passage latitudes.

[30] The northern limit of the wind stress integration area has been defined in this study using the surface layer thickness field, since this is the natural choice of variable to identify the region of circumpolar flow in a reduced-gravity model. The region could be identified in a more complex numerical model, or from observations, using drifters or sea surface height.

[31] A limitation of the reduced-gravity model is that the scaling for diapycnal upwelling velocity leads to large upwelling near the southern boundary, where h is small. The net effect is weak since the deepening of the surface layer is counteracted by local relaxation of h to 10 m, but the large diapycnal fluxes near the southern boundary may contribute to the slight discrepancy between the model result and theory.

[32] An important caveat is the assumption that Southern Ocean eddies can be represented using the scaling of *Gent and McWilliams* [1990], with an isopycnal diffusivity that is independent of the mean flow. The ocean eddy field

almost certainly exhibits threshold behaviour, with changes in eddy kinetic energy causing the ACC to become saturated to changes in wind stress [e.g., *Straub*, 1993; *Tansley and Marshall*, 2001; *Hallberg and Gnanadesikan*, 2006]. While the relationship between wind stress and ACC transport will be more complicated in an eddy-saturated regime, our conclusion that the ACC is driven by winds over the circumpolar streamlines is likely to be robust.

[33] **Acknowledgments.** This study is funded by the UK Natural Environment Research Council. H.L.J. is supported by a Royal Society University Research Fellowship. D.P.M. is supported by the James Martin 21st Century School, University of Oxford. We thank two reviewers for their helpful feedback.

References

Allison, L. C. (2009), Spin-up and adjustment of the Antarctic Circumpolar Current and global pycnocline, Ph.D. thesis, Dep. of Meteorol., Univ. of Reading, Reading, U. K.

Fučkar, N. S., and G. K. Vallis (2007), Interhemispheric influence of surface buoyancy conditions on a circumpolar current, *Geophys. Res. Lett.*, *34*, L14605, doi:10.1029/2007GL030379.

Gent, P. R., and J. C. McWilliams (1990), Isopycnal mixing in ocean circulation models. *J. Phys. Oceanogr.*, *20*, 150–155.

Gill, A. E. (1968), A linear model of the Antarctic Circumpolar Current, *J. Fluid Mech.*, *32*, 465–488.

Gnanadesikan, A. (1999), A simple predictive model for the structure of the oceanic pycnocline, *Science*, *283*, 2077–2079.

Gnanadesikan, A., A. M. de Boer, and B. K. Mignone (2007), A simple theory of the pycnocline and overturning revisited, in *Ocean Circulation: Mechanisms and Impacts*, *Geophys. Monogr. Ser.*, vol. 173, edited by A. Schmittner, J. C. H. Chiang, and S. R. Hemming, pp. 19–32, AGU, Washington, D. C.

Hallberg, R., and A. Gnanadesikan (2006), The role of eddies in determining the structure and response of the wind-driven southern hemisphere overturning: Results from the Modeling Eddies in the Southern Ocean (MESO) project, *J. Phys. Oceanogr.*, *36*, 2232–2252.

Hughes, C. W., M. P. Meredith, and K. J. Heywood (1999), Wind-driven transport fluctuations through Drake Passage: A southern mode, *J. Phys. Oceanogr.*, *29*, 1971–1992.

Kistler, R., et al. (2001), The NCEP-NCAR 50-year reanalysis: Monthly means CD-ROM and documentation, *Bull. Am. Meteorol. Soc.*, *82*, 247–268.

Marshall, J., A. Adcroft, C. Hill, L. Perelman, and C. Heisey (1997), A finite-volume, incompressible Navier Stokes model for studies of the ocean on parallel computers, *J. Geophys. Res.*, *102*, 5753–5766.

Russell, J. L., R. J. Stouffer, and K. W. Dixon (2006), Intercomparison of the Southern Ocean circulations in IPCC coupled model control simulations, *J. Clim.*, *19*, 4560–4575.

Straub, D. N. (1993), On the transport and angular momentum balance of channel models of the Antarctic Circumpolar Current, *J. Phys. Oceanogr.*, *23*, 776–782.

Tansley, C. E., and D. P. Marshall (2001), On the dynamics of wind-driven circumpolar currents, *J. Phys. Oceanogr.*, *31*, 3258–3273.

Toggweiler, J. R., and B. Samuels (1995), Effect of Drake Passage on the global thermohaline circulation, *Deep Sea Res., Part I*, *42*, 477–500.

Trenberth, K. E., W. G. Large, and J. G. Olson (1990), The mean annual cycle in global ocean wind stress, *J. Phys. Oceanogr.*, *20*, 1742–1760.

L. C. Allison, Department of Meteorology, University of Reading, Reading, RG6 6BB, UK. (l.c.allison@reading.ac.uk)

H. L. Johnson, Department of Earth Sciences, University of Oxford, Oxford, OX1 3PR, UK.

D. P. Marshall and D. R. Munday, Atmospheric, Oceanic and Planetary Physics, University of Oxford, Oxford, OX1 3PU, UK.